Supplemental Information

Redox-Responsive Dual Chemo-photothermal Therapeutic Nanomedicine for Imaging-Guided Combinational Therapy

Fei Yu,[a,#] Fuwu Zhang,[d,#] Longguang Tang,[a,#] Jingwen Ma,[b] Daishun Ling,[c] Xiaoyuan Chen,[d,*] and Xiaolian Sun[b,*]

[a]State Key Laboratory of Molecular Vaccinology and Molecular Diagnostics & Center for Molecular Imaging and Translational Medicine, School of Public Health, Xiamen University, Xiamen 361005, China.

[b]State key Laboratory of Natural medicines, Department of Pharmaceutical Analysis, China Pharmaceutical University, Nanjing 210009, China. Email: xiaolian-Sun@cpu.edu.cn

[c]Zhejiang Province Key Laboratory of Anti-Cancer Drug Research, College of Pharmaceutical Sciences, Zhejiang University, Hangzhou 310058, China

[d]Laboratory of Molecular Imaging and Nanomedicine (LOMIN), National Institute of Biomedical Imaging and Bioengineering (NIBIB)

National Institutes of Health

Bethesda, Maryland 20892, United States

Email: shawn.chen@nih.gov

#These authors contributed equally to this paper.

MATERIALS AND METHODS

Materials

Poly lactide-co-glycolide (50:50) (PLGA), Thiophene-2-thiol, 4,6-diamidino-2-phenylindole (DAPI), Indocyanine green (ICG), 4-nitrophenyl chloroformate 3-(4,5-dimethylthiazol-2-yl)-2,5-diphenyltetrazolium bromide (MTT), eosin, propidium iodide (PI), N-hydroxysuccinimide (NHS), (3-Dimethylaminopropyl)-N-ethylcarbodiimide hydrochloride (EDC), Calcein-AM, 4-Dimethylaminopyridine (DMAP) and hematoxylin were obtained from Sigma-Aldrich (USA). 1,2-Distearoyl-sn-glycero-3-phosphoethanolamine-N-[folate (polyethylene glycol)-2000] (DSPE-PEG 2000-FA) and soybean phosphatidylcholine (SPC) were obtained from Avanti (USA). Dialysis bag (Mw = 8000 to 12 000 Da) was purchased from Greenbird Inc. (Shanghai, China). DMEM and fetal bovine serum were bought from Gibco Life Technologies (USA). All other chemicals were purchased from Sigma Aldrich in analytical grade unless noted.

Preparation of CR-(SS-CPT)$_2$

CR and CPT-ss-OH were first synthesized according to our previously reported method. [1, 2] Next, the trimeric prodrug CR-(SS-CPT)$_2$ was synthesized *via* a one-step esterification between the carboxylic acid groups of CR and hydroxyl group of CPT-ss-OH. Briefly, both CR (1 eq.) and excess of CPT-ss-OH (3 eq.) were dissolved in DMSO, followed by addition of EDC (3 eq.) and DMAP (0.5 eq.). The mixture solution was stirred vigorously for 24 h, and precipitated into diethyl ether to remove DMSO. The collected precipitates were further purified by column chromatography on silica gel to obtain a dark solid. ^{1}H NMR (600 MHz, DMSO-d6): δ (ppm) 8.702 (s, 2H), 8.489 (s, 2H), 8.178 (d, J = 8.4 Hz, 2H), 8.136 (d, J= 7.2 Hz, 2H), 7.875 (t, J = 8.4 Hz, 2H), 7.724 (t, J = 7.8 Hz, 2H), 7.089 (s, 2H), 7.036 (s, 2H), 5.433-5.556 (m, 4H), 5.290-

5.345 (m, 2H), 4.331 (t, *J* = 6 Hz, 4H), 3.998 (d, *J* = 13.2 Hz, 4H), 3.505-3.565 (m, 8H), 2.994 (t, J = 7.8 Hz, 4H), 2.768 (t, *J* = 7.8 Hz, 4H), 2.652-2.687 (m, 2H), 2.149-2.221 (m, 4H), 2.044 (d, *J* = 13.8 Hz, 4H), 1.735 (d, *J* = 13.8 Hz, 4H), 0.927 (t, *J* = 7.2 Hz, 6H)

Preparation of FA-CSC-NPs

CR-(SS-CPT)$_2$ loaded nanoparticles (defined as FA-CSC-NPs) were prepared by a modified solvent evaporation method.[3] Firstly, The CR-(SS-CPT)$_2$ and PLGA polymer was added to 2 mL of organic solvent (45% methanol + 55% DCM), following with gentle agitation until a clear solution was achieved. Secondly, the solution was added into 10 mL aqueous solution containing SPC and DSPE-PEG-FA (mass ratio = 2:3). Then, the mixture was emulsified by probe sonication in an ice bath to form a water-in-oil o/w emulsion. The emulsion was stirred overnight and further evaporated under reduced pressure. After washing three times in deionized (DI) water, the FA-CSC-NPs were collected by an Amicon Ultra-4 centrifugal filter (Millipore, Billerica, MA) and kept in DI water for further use. The non-targeting CR-(SS-CPT)$_2$ loaded nanoparticles (defined as CSC-NPs) was prepared in the same method except that the DSPE-PEG-FA was replaced by DSPE-PEG. In addition, CPT loaded nanoparticles (defined as CPT-NPs) and CR loaded nanoparticles (defined as CR-NPs) was also prepared in the same way except that the CR-(SS-CPT)$_2$ was replaced by CPT or CR respectively.

Characterization of FA-CSC-NPs

The zeta potential and hydrodynamic size of FA-CSC-NPs were determined using the Malvern Zeta-sizer Nano-ZS (Malvern Instruments, Worcestershire, UK). The measurements were conducted in triplicate at 25 °C. The morphology and size of the FA-CSC-NPs was analyzed by transmission electron microscope (TEM, JEM 1400, JEOL, Tokyo, Japan). The

sample was placed onto the copper grids and air-dried prior to image acquisition. The surface morphology of FA-CSC-NPs, coating with platinum, was examined by SEM (LEO 1530VP, Oberkochen, Germany). The absorbance and fluorescent spectrums were measured using UV-Vis Spectrophotometer (UV2600, Shimadzu) and Fluorescence Spectrophotometer (LS 55, Perkin Elmer), respectively.

The entrapment efficiency (EE) and drug-loading (DL) capacity were calculated by the following equations and the amount of CPT were measured by high performance liquid chromatography (HPLC).[4]

$$\text{EE (\%)} = \frac{\text{weight of CR-SS-CPT in nanoparticles}}{\text{weight of CR-SS-CPT fed initially}} \times 100\ \%$$

$$\text{DL (\%)} = \frac{\text{weight of CR-SS-CPT in nanoparticles}}{\text{weight of CR-SS-CPT in nanoparticles} + \text{weight of carriers}} \times 100\ \%$$

The photostabilities of FA-CSC-NPs, CSC-NPs, and free ICG were evaluated under laser irradiation (1.0 W/cm^2, 808 nm) for 10 min. The profiles of temperature change was recorded by a thermal camera. Additonlly, the photothermal conversion efficiency (η_T) of CR-(SS-CPT)$_2$ was calculated based on the following equation.[5]

$$\eta_T = \frac{hA(T_{\max} - T_{amb}) - Q_0}{I(1-10^{-A_\lambda})}$$

Where h is the heat transfer coefficient, A is the surface area of the solution, T_{max} is the maximum system temperature, T_{amb} is the surrounding temperature, I refer to the laser power and A_λ refer to the absorbance of solution, Q_0 is defined as the rate of heat input due to light absorption by the solvent.

Drug release

The drug release was analyzed using a dialysis method.[6] Briefly, FA-CSC-NPs aqueous solution was placed in a dialysis tube (MWCO 8000-12000 Da), which was then immersed in 30 mL of different media and shaken at a speed of 100 rpm at 37 °C. At desired intervals, 1.0 mL of release media was taken out and replenished with equal volume of fresh media. The sample solution was analyzed by reverse phase HPLC. The mobile phase was a mixture of 23% acetonitrile and77% aqueous buffer (0.1 M triethylamine acetate buffer, pH = 6) and delivered at a flow rate of 1.0 mL/min. Eluted solutions were measured by absorption at 368 nm with UV–Vis detector. Values were reported as the means for each triplicated sample. Means and corresponding standard deviations (mean ± SD) were shown as results.

***In vitro* cellular uptake**

MCF-7 cells were seeded at a density of 5×10^4 cells chamber with coverglasses.[7] After 24 h incubation, free CR-$(SS\text{-}CPT)_2$, FA-CSC-NPs, CSC-NPs, or FA-CSC-NPs + free FA (200 μg/mL) at equivalent concentration of CR-$(SS\text{-}CPT)_2$ (10 μM)were added respectively and incubated for another 2h. Afterwards, the cells were fixed with 4% paraformaldehyde for 15 min. The cells were further washed with cold PBS and examined by a Leica TCS SP5 confocal laser scanning microscopy (CLSM) (Leica Microsystems, Germany). Besides, the in vitro cellular uptake study of FA-CSC-NPs was also conducted in the MCF-10A (breast epithelial) cells in the same method.

Flow cytometry analysis

Cell uptake was quantitatively analyzed with flow cytometer. MCF-7 cells were seeded in 24-well plate (4×10^5 cells/well) and cultured overnight before they were treated with different

samples at equivalent concentration of CR-(SS-CPT)$_2$ (10 μM) for 2h. Lastly, the cells were trypsinized, washed with PBS, and resuspended in PBS. The cellular fluorescence intensity of CPT was recorded using a FACS Calibr flow cytometer (Becton Dickinson, USA).

***In vitro* cytotoxicity**

MCF-7 cells were seeded in 96-well plates at a density of 1.0×10^4 cells per well. After culture for 24 h, the cells were treated with free CR-(SS-CPT)$_2$, FA-CSC-NPs, or CSC-NPs with or without NIR laser irradiation (5 min, 1 W/cm^2). The NPs were equivalent to the corresponding concentrations of free CR-(SS-CPT)$_2$. The concentrations of CR-(SS-CPT)$_2$ were set as 0.23, 0.46, 0.92, 1.83, 3.75, 7.5, 15, 30 μM. After 24 h incubation, the cell viability was evaluated using MTT assay. The half-maximal inhibitory concentrations (IC_{50}) were calculated by SPSS 12.0 software. The calcein acetoxymethyl ester (calcein-AM) and propidium iodide (PI) staining was carried out according to the manufacturer's suggested protocol. In addition, in order to further investigate the selective cytotoxicity of FA-CSC-NPs, the MTT assay was also conducted in the MCF-10A cells in the same way.

In Vivo Pharmacokinetic of the FA-CSC-NPs.

Sprague-Dawley rats (200 ± 20 g) were divided into 2 groups at random (n = 5 for each group) to investigate the pharmacokinetics of FA-CSC-NPs and CR-(SS-CPT)$_2$. The rats were injected with a single dose of 5 mg/kg (CR-(SS-CPT)$_2$ equivalent) of drug-loaded formulations via the tail vein. Orbital blood samples (0.5 mL) were collected into heparinized tubes at appropriate intervals post-injection. Whole blood was immediately processed for harvesting the plasma by centrifugation at 4000 rpm for 10 min. The plasma was stored at -80 °C until required for HPLC analysis. The pharmacokinetic parameters were calculated by the WinNonlin Professional

Edition Version 2.1 (Pharsight Corporation, Mountain View, California). All the animal procedures were performed in accordance with the guidelines of the Xiamen University Institutional Animal Care and Use Committee.

Biodistribution

The tumor bearing mice were constructed *via* the subcutaneous injection of MCF-7 cells into female BALB/c mice (~20 g). Then, the mice were intravenously injected by FA-CSC-NPs or CSC-NPs at equivalent CR-$(SS\text{-}CPT)_2$ concentration. *In vivo* NIRF images and PA images were obtained at 1.5, 3, 6, 12, and 24 h post-injection using IVIS Lumina imaging system (Caliper Life Sciences, USA) and Endra Nexus 128 system respectively. The mice were euthanized at 24 h post-injection. Then, various tissues including heart, liver, spleen, lung, kidney and tumor were extracted from the mice and finally imaged and analyzed by Living Image Software.

***In vivo* infrared thermal imaging and anticancer effect**

When tumor volumes approached ~80 mm^3, the mice were used for infrared thermal imaging. The mice were *i.v.* injected with 200 μL of PBS, free CR-$(SS\text{-}CPT)_2$, CSC-NPs and FA-CSC-NPs at equivalent concentration of CR-$(SS\text{-}CPT)_2$ (5 mg/kg), respectively. At 12 h post-injection, the tumor sites were exposure to the 808 nm laser irradiation (1 W/cm^2) for 5 min. During laser irradiation, region maximum temperatures and infrared thermographic maps were obtained with the infrared thermal imaging camera.

In addition, when the tumors reached to ~100 mm^3, the mice were divided into eight groups randomly: (a) PBS group as the control, (b) PBS + laser group, (c) free CR-$(SS\text{-}CPT)_2$ group, (d) free CR-$(SS\text{-}CPT)_2$ + laser group, (e) CSC-NPs group, (f) CSC-NPs + laser group, (g) FA-CSC-NPs group, and (h) FA-CSC-NPs + laser group. For the laser treatment groups, the tumors were

exposed to the NIR laser at 1 W/cm^2 for 5 min. The tumor size of each mouse was recorded. Meanwhile, the body weights of each group were also recorded up to 2 weeks. For the hematoxylin and eosin (H&E) staining, the formalin-fixed main organs were embedded in paraffin blocks, sectioned at 8 mm, stained with H&E, and examined by optical microscope (DM5500B, Leica Microsystems, Germany).

Statistical analysis

The two-tailed Student's t-test was performed to analyze the statistical significance of different groups. Data are presented as mean ± SD. A difference was considered statistically significant when the P value fell below 0.05.

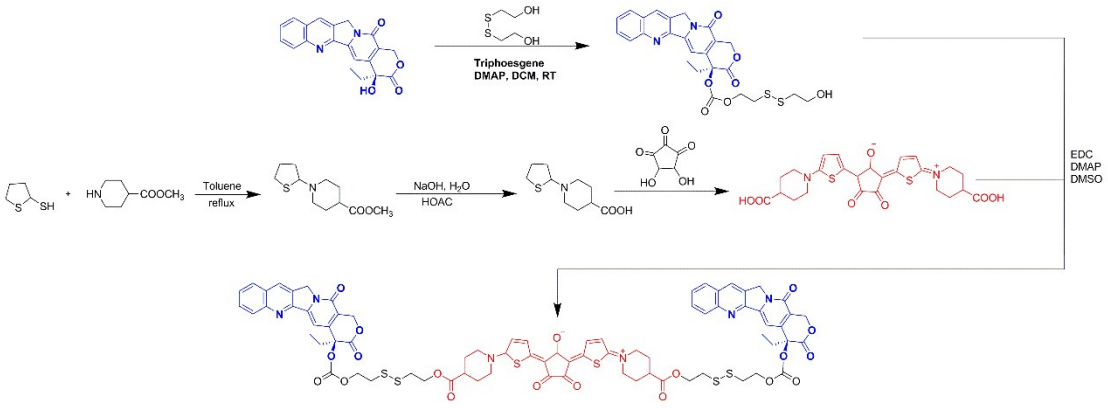

Figure S1. Synthetic route of CR-(SS-CPT)$_2$.

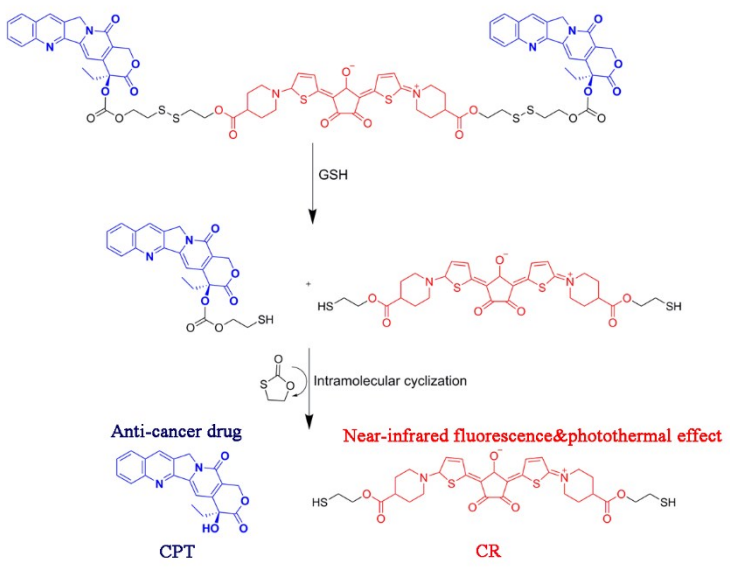

Figure S2. Proposed CPT release mechanism of the activatable prodrug with the presence of GSH.

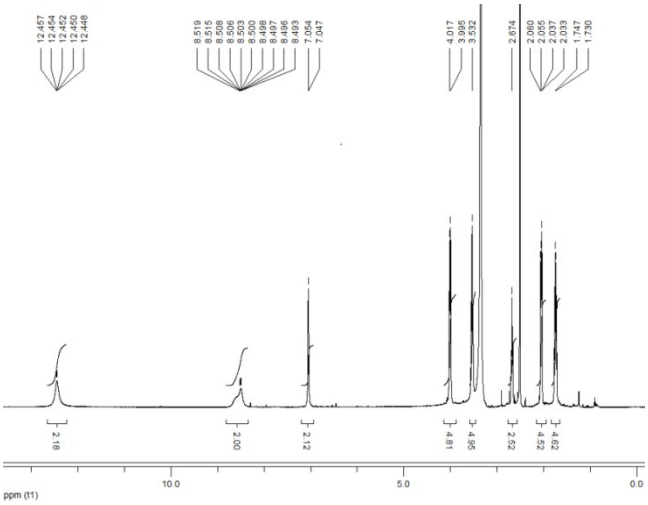

Figure S3. ^{1}H NMR spectrum of CR in DMSO-d_6.

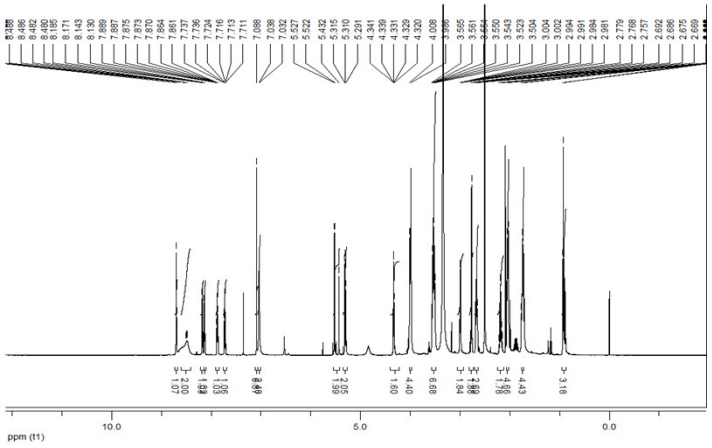

Figure S4. ^{1}H NMR spectrum of CR-(SS-CPT)$_2$ in DMSO-d$_6$.

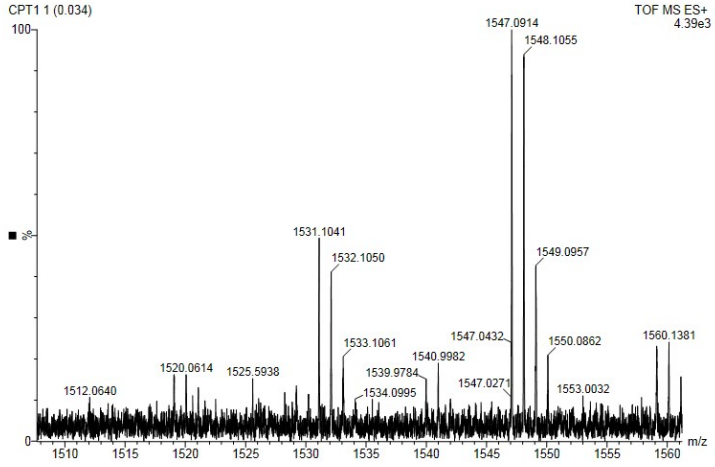

Figure S5. HRMS spectrum of CR-(SS-CPT)$_2$.

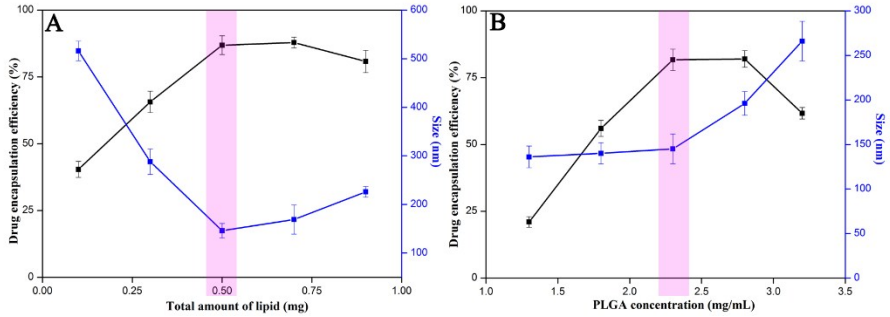

Figure S6. The effects of (A) total amount of lipid and (B) polymer concentration on the size and EE (n = 3). The final optimized mass ratio is CR-(SS-CPT)$_2$: PLGA: SPC: DSPE-PEG-FA = 0.99 : 4.6 : 0.2 : 0.3.

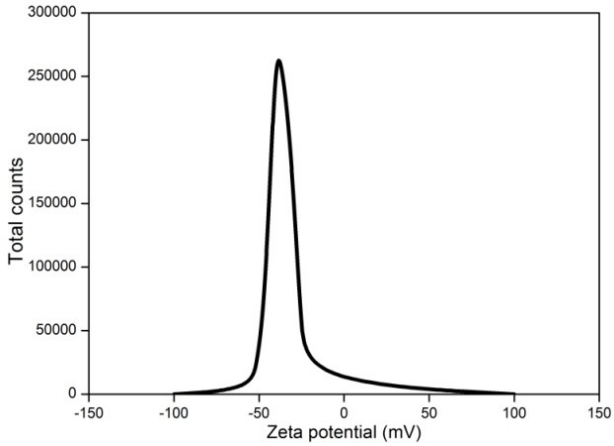

Figure S7. Zeta potential of the FA-CSC-NPs.

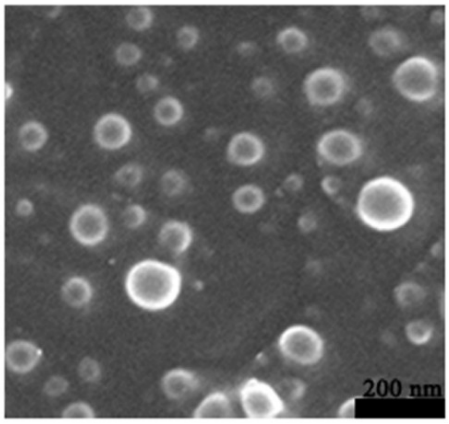

Figure S8. SEM image of the FA-CSC-NPs.

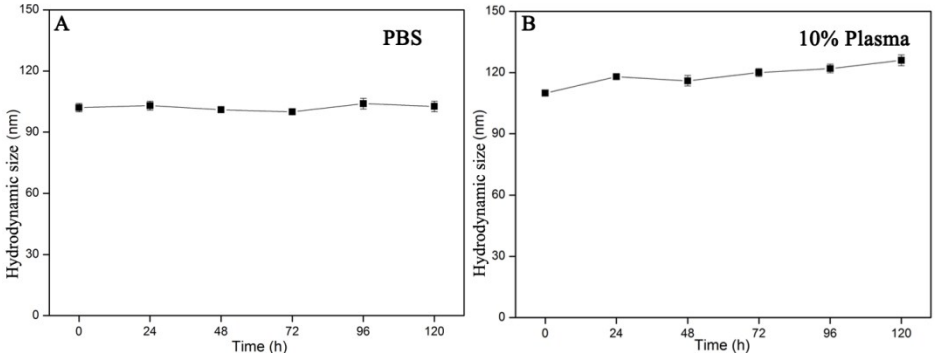

Figure S9. *In vitro* stability of the FA-CSC-NPs in PBS or 10% plasma for 120 h (mean ± SD, n=3).

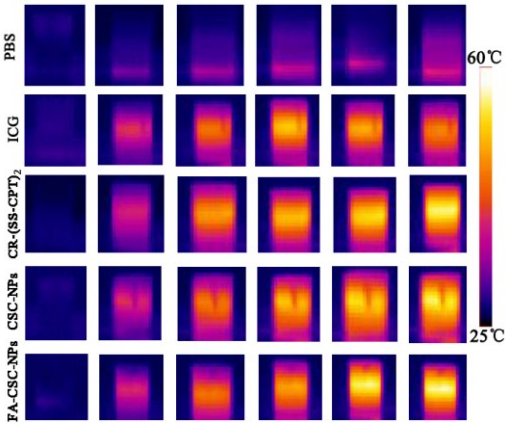

Figure S10. Infrared thermographic images of PBS, free ICG, CR-$(SS\text{-}CPT)_2$, CSC-NPs and FA-CSC-NPs under 808 nm laser irradiation (1 W/cm^2, 5 min).

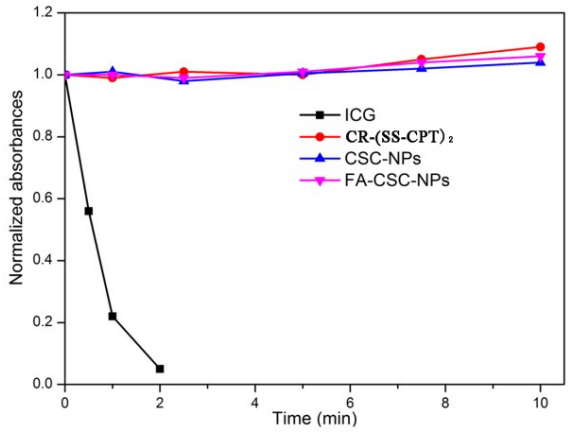

Figure S11. Normalized absorbance of ICG, CR-(SS-CPT)$_2$, CSC-NPs and FA-CSC-NPs at various time under 808 nm laser irradiation.

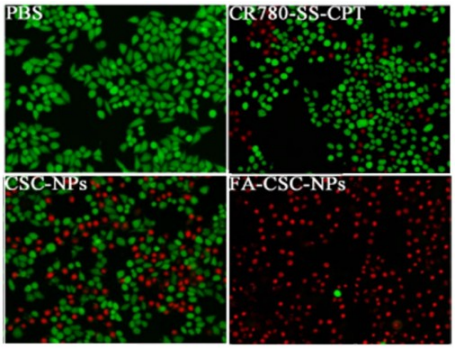

Figure S12. Calcine AM/PI staining of MCF-7 cells treated with PBS, free CR-(SS-CPT)$_2$, CSC-NPs, and FA-CSC-NPs with 808-nm laser irradiation (1 W/cm^2, 5 min).

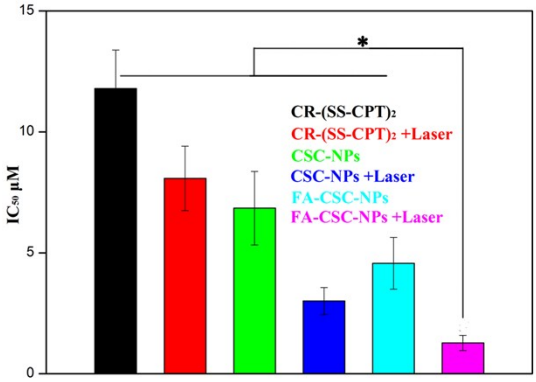

Figure S13. The statistical analysis of IC$_{50}$ values with each groups.

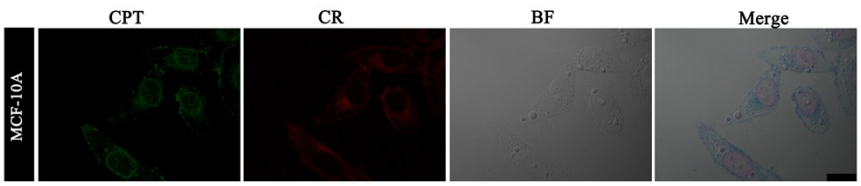

Figure S14. Confocal images of MCF-10A cells incubated with FA-CSC-NPs. (scale bar = 20 μm).

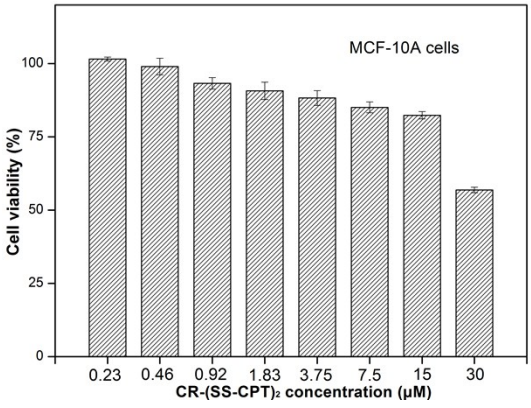

Figure S15. Cytotoxicity evaluation of FA-CSC-NPs incubated in MCF-10A cells.

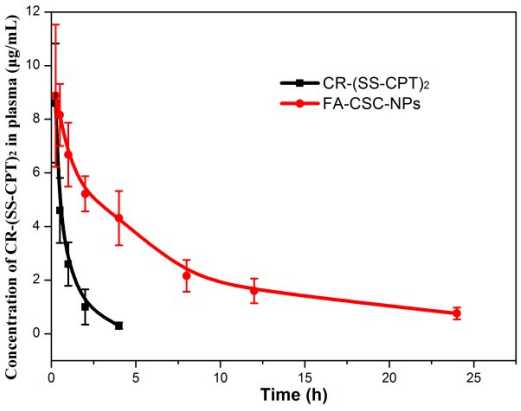

Figure S16. *In vivo* pharmacokinetic profile of the FA-CSC-NPs and CR-$(SS\text{-}CPT)_2$.

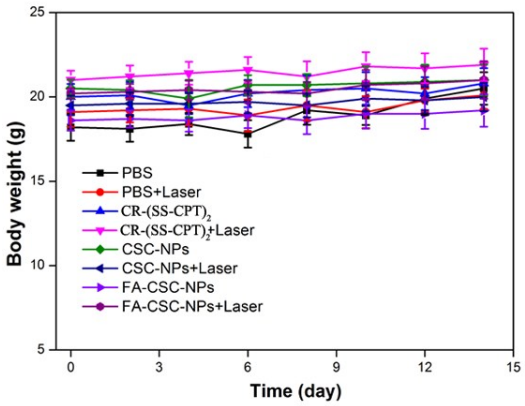

Figure S17. Body weight change of the mice injected with PBS, free CR-(SS-CPT)$_2$, CSC-NPs, and FA-CSC-NPs with/without 808 nm laser irradiation (1 W/cm^2, 5 min).

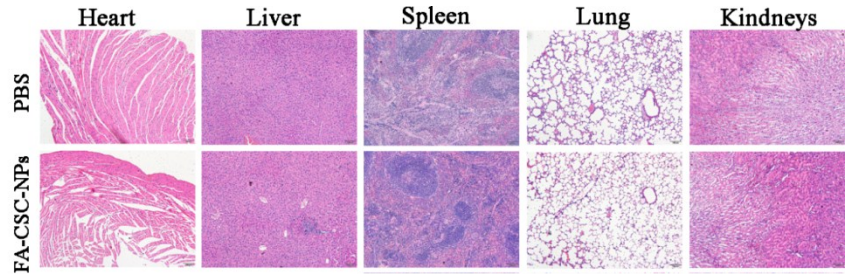

Figure S18. Representative H&E stained images of major organs including the heart, liver, spleen, lung and kidney collected from the mice after 14 days post-injection of FA-CSC-NPs and PBS plus laser irradiation.

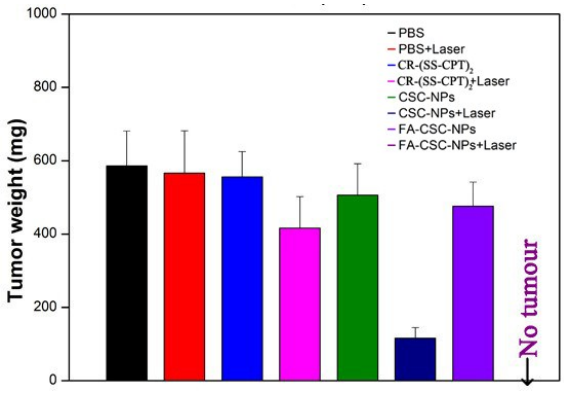

Figure S19. Tumor weight of the mice injected with PBS, free CR-(SS-CPT)$_2$, CSC-NPs, and FA-CSC-NPs with/without 808-nm laser irradiation (1 W/cm^2, 5 min).

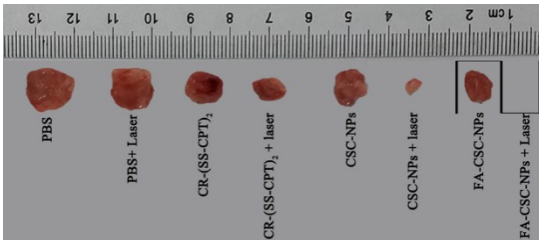

Figure S20. Representative image of the tumors at the end of various therapies.

Table S1. Pharmacokinetic parameters of CR-(SS-CPT)$_2$ in rats after intravenous administration of FA-CSC-NPs and CR-(SS-CPT)$_2$.

	$t_{1/2}$ (h)	$AUC_{0-\infty}$ (mg*h*L^{-1})	$MRT_{0-\infty}$ (h)	CL (L*h^{-1})
CR-(SS-CPT)$_2$	0.49 ± 0.13	8.02 ± 2.93	1.17 ± 0.15	0.69 ± 0.27
FA-CSC-NPs	4.17 ± 0.15*	68.83 ± 16.93*	12.57 ± 0.6*	0.08 ± 0.02*

*P < 0.05 vs. CR-(SS-CPT)$_2$

■ REFERENCES

1. F. Zhang, G. Zhu, O. Jacobson, Y. Liu, K. Chen, G. Yu, Q. Ni, J. Fan, Z. Yang, F. Xu, X. Fu, Z. Wang, Y. Ma, G. Niu, X. Zhao and X. Chen, *ACS Nano.*, 2017, **11**, 8838-8848.
2. L. Tang, F. Zhang, F. Yu, W. Sun, M. Song, X. Chen, X. Zhang and X. Sun, *Biomaterials*, 2017, **129**, 28-36.
3. G. Cavallaro, E. F. Craparo, C. Sardo, G. Lamberti, A. A. Barba and A. Dalmoro, *Int. J. Pharm.*, 2015, **495**, 719-727.
4. L. Qiu, Z. Li, M. Qiao, M. Long, M. Wang, X. Zhang, C. Tian and D. Chen, *Acta.Biomater.*, 2014, **10**, 2024-2035.
5. J. Cui, S. Xu, C. Guo, R. Jiang, T. D. James and L. Wang, *Anal. Chem.*, 2015, **87**, 11592-11598.
6. K. Avgoustakis, A. Beletsi, Z. Panagi, P. Klepetsanis, A. G. Karydas and D. S. Ithakissios, *J. Control. Release.*, 2002, **79**, 123-135.
7. M. Zheng, P. Zhao, Z. Luo, P. Gong, C. Zheng, P. Zhang, C. Yue, D. Gao, Y. Ma and L. Cai, *ACS Appl. Mater. Interfaces*, 2014, **6**, 6709-6716.